

Resistance and Reactance of Monopole Fields Induced by a Test Charge Drifting Off-Axis in a Cold and Collisional Cylindrical Plasma *

M. S. Bawa'aneh^{1**}, A. M. Al-Khateeb¹, Y. -c. Ghim²

¹Department of Physics, Yarmouk University, Irbid, Jordan

²Department of Nuclear and Quantum Engineering, KAIST, Daejeon, Korea

(Received 9 January 2018)

We study the interaction of a uniform, cold and collisional plasma with a test charged particle moving off-axis at a constant speed down a cylindrical tube with a resistive thick metallic wall. Upon matching the electromagnetic field components at all interfaces, the induced monopole electromagnetic fields in the plasma are obtained in the frequency domain. An expression for the plasma electric resistance and reactance is derived and analyzed numerically for some representative parameters. Near the plasma resonant frequency, the plasma resistance evolves with frequency like a parallel RLC resonator with peak resistance at the plasma frequency ω_{pe} , while the plasma reactance can be capacitive or inductive in nature depending on the frequency under consideration.

PACS: 51.50.+v, 52.50.Gj, 52.50.Sw, 52.25.Mq

DOI: 10.1088/0256-307X/35/8/085101

Growing waves could be generated in plasma by injecting charged particles at a velocity near the plasma wave phase velocity. In the plasma microwave-frequency spectrum, the motion of the plasma ions is not important and it is convenient to treat the ions as a neutralizing background of positive charge. In the simplified treatment of a plasma as a dielectric medium, convection currents resulting from the plasma electrons and ions are accounted for in the derivation of the equivalent dielectric permittivity tensor $\vec{\epsilon}$.^[1–3] In general, the plasma becomes an anisotropic medium when its electric properties vary with direction. For example, in the presence of an external magnetic field, the plasma particles gyrate about the field lines in one direction, and therefore make the plasma behave like an anisotropic dielectric with an equivalent dielectric tensor, which accounts for such anisotropy.

It is well known that electromagnetic waves cannot propagate in an overdense plasma if the plasma frequency is above the excitation frequency. Waves are reflected at the bulk plasma frequency and become evanescent waves.^[4–6] This may give rise to heating of the plasma and then waves do not travel any more in the radial direction, but rather propagate along the plasma-vacuum or plasma-metal interfaces. The wave energy is then transferred to the plasma by the evanescent wave, which enters the plasma perpendicular to its surface and decays exponentially.

In a collisionless cold plasma, waves are reflected at the bulk plasma frequency ω_{pe} . There will be a stopband for wave propagation for frequencies below ω_{pe} , and a passband for $\omega > \omega_{pe}$.^[1,6] In the presence of collisions, the propagation characteristics are altered considerably if the collision frequency ν approaches or surpasses the plasma frequency. Higher collision frequencies can lead to stronger reflection and weaker absorption. Waves are then allowed to propagate in the plasma at frequencies below ω_{pe} and the stopband

becomes narrower as ν increases and disappears at $\omega_{pe} \approx \nu$. For $\nu > \omega_{pe}$ there will be no stopband, and waves will propagate, although attenuated, at all frequencies.^[1,3]

The monopole longitudinal effects of a homogeneous, cold, and collisional plasma, which is filling the interior of a resistive cylindrical tube, are considered in the present work. Knowing the plasma response as a dielectric medium to an external excitation by finding the resistance and reactance of the plasma as functions of source-plasma-environment parameters allows for a better choice of the configuration of a microwave-plasma transmission system to couple waves to plasmas with high efficiency.^[7–12]

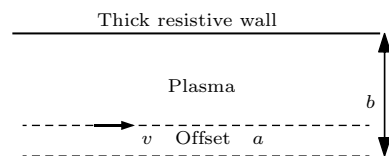


Fig. 1. Plasma-pipe geometry.

Cold plasmas compared with metals are considered as poor conductors and are often used for propagation of high-current particle beams. Plasma impedance can lead to returning current perturbations, which interrupt the directed plasma electron motion.^[13] In accelerators, electron clouds may be idealized as cold uniformly distributed nonneutral plasmas, which affect the dynamics of beams and their wakefields, and finally the coupling impedance of such fields to their environment.^[14,15] Such clouds can be generated in the pipe due to the ionization of the residual gas that may accumulate to a certain level.^[16] Resistance results from collisions that interrupt the directed plasma electron motion. Collisions with neutrals are important in weakly ionized plasmas at high current density electrons and can exchange momentum with plasma ions through collective instabilities.

*Supported by the Yarmouk University, and the KUSTAR–KAIST Institution Fund.

**Corresponding author. Email: msbawaaneh@yu.edu.jo

© 2018 Chinese Physical Society and IOP Publishing Ltd

We consider a test particle of charge q_0 at position $r = a$, which travels at velocity $v\hat{z}$ down a cylindrical pipe of radius b , as shown in Fig. 1. We assume an isotropic collisional and unmagnetized plasma filling the cylindrical pipe. The corresponding lowest monopole charge and current densities are^[17–19]

$$\rho_0(\mathbf{r}, t) = \frac{q_0}{2\pi r} \delta(r-a) \delta(z-\beta ct), \quad \mathbf{J}_0(\mathbf{r}, t) = \rho_0 \beta c \hat{z}, \quad (1)$$

where c is the speed of light in free space, and $\beta = v/c$ is the relativistic factor. Upon treating the plasma as an isotropic dielectric medium in the absence of an external magnetic field, and by combining Maxwell's curl equations for a medium with conductivity g , we obtain the following general equation that governs the electric field with $\hat{O}_1 = \nabla^2 - \mu_0 g \frac{\partial}{\partial t} - \mu_0 \epsilon_0 \epsilon \frac{\partial^2}{\partial t^2}$,

$$\hat{O}_1 \mathbf{E}(\mathbf{r}, t) - \nabla(\nabla \cdot \mathbf{E}(\mathbf{r}, t)) = \mu_0 \frac{\partial \mathbf{J}_0(\vec{r}, t)}{\partial t}, \quad (2)$$

where ϵ is the longitudinal dielectric function, and μ_0 and ϵ_0 are the permeability and permittivity of the vacuum, respectively. Fourier time-transform of the wave equation for the electric field results in the following equation in the frequency domain with $\hat{O}_2 = \nabla^2 - j\mu_0 g \omega + \frac{\omega^2 \epsilon}{c^2}$,

$$\hat{O}_2 \mathbf{E}(\mathbf{r}, \omega) - \nabla(\nabla \cdot \mathbf{E}(\mathbf{r}, \omega)) = \frac{j\mu_0 \omega q_0 \delta(r-a) e^{-j\frac{\omega z}{\beta c}} \hat{z}}{2\pi r}. \quad (3)$$

The z -components of Eq. (3) in each region of interest take on the following forms

$$\begin{aligned} & \left[\nabla^2 + \frac{\omega^2}{c^2} \epsilon_p \right] E_z^{(1)}(\mathbf{r}, \omega) - \frac{\partial}{\partial z} (\nabla \cdot \mathbf{E}(\mathbf{r}, \omega)) \\ & = j\mu_0 \omega \frac{q_0}{2\pi r} \delta(r-a) e^{-j\frac{\omega z}{\beta c}}, \quad 0 \leq r \leq a. \end{aligned} \quad (4)$$

For $a \leq r \leq b$, $E_z(\mathbf{r}, \omega) = E_z^{(2)}(\mathbf{r}, \omega)$, and for $b \leq r < \infty$, $E_z(\mathbf{r}, \omega) = E_z^{(3)}(\mathbf{r}, \omega)$, we have

$$\begin{aligned} & \left[\nabla^2 + \frac{\omega^2}{c^2} \epsilon_p \right] E_z^{(2)}(\mathbf{r}, \omega) - \frac{\partial}{\partial z} (\nabla \cdot \mathbf{E}(\mathbf{r}, \omega)) = 0, \quad (5) \\ & \left[\nabla^2 - j\mu_0 g \omega + \frac{\omega^2}{c^2} \right] E_z^{(3)}(\mathbf{r}, \omega) - \frac{\partial}{\partial z} (\nabla \cdot \mathbf{E}(\mathbf{r}, \omega)) = 0, \quad (6) \end{aligned}$$

where ϵ_p is the longitudinal dielectric function inside the plasma. Here we set the longitudinal dielectric function in the metallic wall as $\epsilon = 1$. For the isotropic, cold, and unmagnetized plasma we have^[1]

$$\epsilon_p = 1 + \frac{\omega_{pe}^2}{j\omega(\nu + j\omega)}, \quad (7)$$

where ω_{pe} is the electron plasma frequency, and ν is the effective collision frequency, which accounts for damping effects. Formulae of the dielectric function for magnetized plasma both with and without the thermal effect, similar to that of Eq. (7), can be found in the literature.^[20–23]

Since the monopole charge and current densities corresponding to the test particle are rotationally symmetric, only transverse-magnetic (TM) cylindrical waveguide modes couple to the fields excited by the test particle such that $B_z = 0$.^[24,25] The lowest transverse electric (TE) mode with $E_z = 0$ has a transverse electric dipole field and thus does not have to be considered here due to the decoupling of this mode from the source (wave equation for B_z is source free). All other field components are obtained from $E_z(r, z, \omega)$ via Maxwell's equations, where E_θ and B_r vanish identically because of axial symmetry and periodicity.

For field variations with z in the frequency domain such as $e^{-j\frac{\omega z}{\beta c}}$, and making use of Maxwell's curl equations, we find the following general relations between the longitudinal electric field component $E_z(r, z, \omega)$ and the non-vanishing transverse field components $E_r(r, z, \omega)$ and $B_\theta(r, z, \omega)$,

$$E_r^{(1,2)}(r, z, \omega) = j \frac{\beta c}{\omega} \frac{1}{1 - \beta^2 \epsilon_p} \frac{dE_z^{(1,2)}(r, z, \omega)}{dr}, \quad (8)$$

$$E_r^{(3)}(r, z, \omega) = j \frac{\beta c}{\omega} \frac{1}{1 - \beta^2 + j \frac{\beta^2 g}{\omega \epsilon_0}} \frac{dE_z^{(3)}(r, z, \omega)}{dr}, \quad (9)$$

$$B_\theta^{(1,2)}(r, z, \omega) = j \frac{\beta^2 \epsilon_p}{\omega(1 - \beta^2 \epsilon_p)} \frac{dE_z^{(1,2)}(r, z, \omega)}{dr}, \quad (10)$$

$$B_\theta^{(3)}(r, z, \omega) = j \frac{\beta^2(1 - j \frac{g}{\omega \epsilon_0})}{\omega(1 - \beta^2 + j \frac{\beta^2 g}{\omega \epsilon_0})} \frac{dE_z^{(3)}(r, z, \omega)}{dr}. \quad (11)$$

$$E_\theta^{(1,2,3)}(r, z, \omega) = B_r^{(1,2,3)}(r, z, \omega) = 0. \quad (12)$$

For $\gamma_0^{-2} = 1 - \beta^2$, $\sigma_0 = \omega/\beta\gamma_0 c$, and upon introducing σ_c and σ_p such that

$$\sigma_c^2 = \frac{\omega^2}{\beta^2 c^2} \left(1 - \beta^2 + j \frac{\beta^2 g}{\omega \epsilon_0} \right) = \sigma_0^2 \left(1 + j \frac{\beta^2 \gamma_0^2 g}{\omega \epsilon_0} \right), \quad (13)$$

$$\begin{aligned} \sigma_p^2 &= \frac{\omega^2}{\beta^2 c^2} \left(1 - \beta^2 - \frac{\beta^2 \omega_p^2}{j\omega(\nu + j\omega)} \right) \\ &= \sigma_0^2 \left(1 - \frac{\gamma_0^2 \beta^2 \omega_p^2}{j\omega(\nu + j\omega)} \right), \end{aligned} \quad (14)$$

the transverse electromagnetic fields in each region become

$$E_r^{(1,2)}(r, z, \omega) = j \frac{k_z}{\sigma_p^2} \frac{dE_z^{(1,2)}(r, z, \omega)}{dr}, \quad (15)$$

$$B_\theta^{(1,2)}(r, z, \omega) = j \frac{\omega \mu_0 \epsilon_0 \epsilon_p}{\sigma_p^2} \frac{dE_z^{(1,2)}(r, z, \omega)}{dr} \quad (16)$$

$$E_r^{(3)}(r, z, \omega) = j \frac{k_z}{\sigma_c^2} \frac{dE_z^{(3)}(r, z, \omega)}{dr}, \quad (17)$$

$$B_\theta^{(3)}(r, z, \omega) = j \frac{\mu_0(\omega \epsilon_0 - jg)}{\sigma_c^2} \frac{dE_z^{(3)}(r, z, \omega)}{dr}. \quad (18)$$

Accordingly, the radial wave equations for the electric field components $E_z^{(1,2,3)} = E_z^{(1,2,3)}(r, z, \omega)$ in the

three regions of interest become

$$\left[\frac{d^2}{dr^2} + \frac{1}{r} \frac{d}{dr} - \sigma_p^2 \right] E_z^{(1)} = - \frac{j\sigma_p^2 q_0 \delta(r-a) e^{-j\frac{\omega z}{\beta c}}}{\omega \epsilon_0 \epsilon_p 2\pi r}, \quad (19)$$

$$\left[\frac{d^2}{dr^2} + \frac{1}{r} \frac{d}{dr} - \sigma_p^2 \right] E_z^{(2)} = 0, \quad (20)$$

$$\left[\frac{d^2}{dr^2} + \frac{1}{r} \frac{d}{dr} - \sigma_c^2 \right] E_z^{(3)} = 0. \quad (21)$$

Due to the presence of ϵ_p^{-1} on the right-hand side of Eq. (19), the formalism of plasmas as dielectric media breaks down at $\omega = \omega_p$ in linear theory in the absence of ν since it leads to unbounded resonant responses. The present problem is dynamical in nature unlike the case of looking for plasma wave propagation characteristics in a conducting pipe. In the static limit $\omega \rightarrow 0$, ϵ_p is divergent, and therefore, the plasma dielectric response can only be defined for time varying processes.

Equation (19) will now be solved using field matching for appropriate boundary conditions at interfaces with the overall regular solution of the wave equation for E_z in each region being

$$E_z(r, z, \omega) = \begin{cases} e^{-j\frac{\omega z}{\beta c}} A_1 I_0(\sigma_p r), & 0 \leq r \leq a, \\ e^{-j\frac{\omega z}{\beta c}} A_2 I_0(\sigma_p r) + A_3 K_0(\sigma_p r), & a \leq r \leq b, \\ e^{-j\frac{\omega z}{\beta c}} A_4 K_0(\sigma_c r), & b \leq r < \infty, \end{cases}$$

where I_0 and K_0 are the zeroth-order modified cylindrical Bessel functions of the first and second kinds, respectively. Integrating Eq. (19) from $r = a - \delta$ to $r = a + \delta$ for vanishingly small δ results in the following boundary condition of the discontinuity of $\partial E_z / \partial r$ at the surface ($r = a$),

$$\left[\frac{\partial E_z^{(2)}}{\partial r} - \frac{\partial E_z^{(1)}}{\partial r} \right]_{r=a} = -j \frac{\sigma_p^2 q_0}{\omega \epsilon_0 \epsilon_p 2\pi a} e^{-j\frac{\omega z}{\beta c}}. \quad (22)$$

Using Eq. (22), the continuity of E_z at $r = a$, and the continuity of E_z and B_θ at $r = b$, we obtain the following system of algebraic equations for the unknown integration constants

$$A_1 I_0(\sigma_p a) = A_2 I_0(\sigma_p a) + A_3 K_0(\sigma_p a), \quad (23)$$

$$A_2 I_1(\sigma_p a) - A_3 K_1(\sigma_p a) - A_1 I_1(\sigma_p a) = \frac{-j\sigma_p q_0}{\omega \epsilon_0 \epsilon_p 2\pi a}, \quad (24)$$

$$A_2 I_0(\sigma_p b) + A_3 K_0(\sigma_p b) = A_4 K_0(\sigma_c b), \quad (25)$$

$$\eta [A_2 I_1(\sigma_p b) - A_3 K_1(\sigma_p b)] = -A_4 K_1(\sigma_c b), \quad (26)$$

where η is defined as

$$\eta = \frac{j\omega \epsilon_0 \epsilon_p \sigma_c}{\sigma_p (g + j\omega \epsilon_0)}. \quad (27)$$

The integration constants $A_{1,2,3,4}$ are obtained by simultaneously solving the system of Eqs. (23)–(26),

$$\text{which yield } A_3 = \frac{j\sigma_p^2 a I_0(\sigma_p a)}{\omega \epsilon_0 \epsilon_{33}} \frac{q_0}{2\pi a},$$

$$A_2 = - \frac{K_0(\sigma_p b) - \eta \frac{K_0(\sigma_c b)}{K_1(\sigma_c b)} K_1(\sigma_p b)}{I_0(\sigma_p b) + \eta \frac{K_0(\sigma_c b)}{K_1(\sigma_c b)} I_1(\sigma_p b)} A_3, \quad (28)$$

$$A_4 = \frac{\eta}{K_1(\sigma_c b)} [K_1(\sigma_p b) + F I_1(\sigma_p b)], \quad (29)$$

$$A_1 = j\sigma_p a \frac{\sigma_p}{\omega \epsilon_0 \epsilon_{33}} \frac{q_0}{2\pi a} [K_0(\sigma_p a) - F I_0(\sigma_p a)], \quad (30)$$

$$F = \frac{K_0(\sigma_p b) - \eta \frac{K_0(\sigma_c b)}{K_1(\sigma_c b)} K_1(\sigma_p b)}{I_0(\sigma_p b) + \eta \frac{K_0(\sigma_c b)}{K_1(\sigma_c b)} I_1(\sigma_p b)}. \quad (31)$$

Using the integration constant A_1 of Eq. (28), the longitudinal electric field $E_z^{(1)} = E_z^{(1)}(r, z, \omega)$ is

$$E_z^{(1)} = \frac{j\sigma_p^2 q_0 e^{-j\frac{\omega z}{\beta c}}}{2\pi \omega \epsilon_0 \epsilon_{33}} [K_0(\sigma_p a) - F I_0(\sigma_p a)] I_0(\sigma_p r). \quad (32)$$

Consider the following frequency domain Maxwell curl equations in terms of electric \mathbf{E} and magnetic \mathbf{H} fields in a linear medium

$$\nabla \times \mathbf{E}(\mathbf{r}, \omega) = -j\mu\omega \mathbf{H}(\mathbf{r}, \omega), \quad (33)$$

$$\nabla \times \mathbf{H}(\mathbf{r}, \omega) = \mathbf{J}(\mathbf{r}, \omega) + j\epsilon_0\omega \overset{\leftrightarrow}{\epsilon} \cdot \mathbf{E}(\mathbf{r}, \omega). \quad (34)$$

Here it is assumed that the permittivity and the permeability are independent of electric and magnetic fields. The total current \mathbf{J} includes only impressed and conduction currents. Effects of possible electric polarization and magnetization are generally included in the permittivity and permeability tensors. In our case, the plasma polarization and axial dc-magnetic field effects are included in the tensor $\overset{\leftrightarrow}{\epsilon}$.

By scalar multiplication of Eq. (33) by $\mathbf{H}^*(\mathbf{r}, \omega)$ and the complex conjugate of Eq. (33) by $\mathbf{E}(\mathbf{r}, \omega)$, the difference of the resulting two equations is

$$\begin{aligned} & \nabla \cdot (\mathbf{E} \times \mathbf{H}^*) \\ &= \mathbf{H}^* \cdot \nabla \times \mathbf{E} - \mathbf{E} \cdot \nabla \times \mathbf{H}^* \\ &= -j\mu\omega \mathbf{H}^* \cdot \mathbf{H} - \mathbf{E} \cdot \mathbf{J}^* + j\epsilon_0\omega \mathbf{E} \cdot \overset{\leftrightarrow}{\epsilon} \cdot \mathbf{E}^* \\ &= -j\omega [\mu \mathbf{H}^* \cdot \mathbf{H} - \epsilon_0 \mathbf{E} \cdot \overset{\leftrightarrow}{\epsilon} \cdot \mathbf{E}^*] - \mathbf{E} \cdot \mathbf{J}^* \\ &\equiv -2j\omega [w_m - w_e] - \mathbf{E} \cdot \mathbf{J}^*, \end{aligned} \quad (35)$$

where w_m and w_e are the magnetic and electric energy densities stored in the system, respectively. With $\mathbf{S} = \mathbf{E} \times \mathbf{H}^*$, Eq. (35) can be rearranged as

$$2j\omega \Delta u_{em} + \nabla \cdot \mathbf{S} = -\mathbf{E} \cdot \mathbf{J}^*, \quad \Delta u_{em} = w_m - w_e, \quad (36)$$

where Δu_{em} is the net electromagnetic energy density stored in the system, and \mathbf{S} is the complex Poynting vector, which is a power surface density measured in Joule per second per meter square. Equation (36) is the complex Poynting's theorem in the differential form, which represents a conservation law of electromagnetic field energy. In integral form, Poynting's theorem of Eq. (36) can be written as

$$2j\omega \int_V d^3r \Delta u_{em} + \oint_{\Omega_s} \mathbf{S} \cdot d\mathbf{a} = - \int_V d^3r \mathbf{E} \cdot \mathbf{J}^*, \quad (37)$$

where Ω_s is the surface enclosing the volume V . For a total current density such that $\mathbf{J}(\mathbf{r}, \omega) = g\mathbf{E}(\mathbf{r}, \omega) + \mathbf{J}_e(\mathbf{r}, \omega)$, we introduce P_0 as the complex power supplied by an impressed current source, P_d as the power converted into heat via the Joule heating, and P_{rad} as the power leaving the region bounded by the surface of integration^[26]

$$P_0 = - \int_V d^3r \mathbf{E} \cdot \vec{J}_e^* \equiv Z(\omega) |I_e(\omega)|^2, \quad (38)$$

$$P_d = \int_V d^3r g E^2, \quad P_{\text{rad}} = \int_S \mathbf{S} \cdot d\mathbf{a}, \quad (39)$$

where $Z(\omega)$ represents a field defined electric impedance of the system, and $I_e(\omega)$ is the spectral current corresponding to the off-axis test charge. Solving Eq. (37) for $Z(\omega)$, we obtain

$$Z(\omega) = \frac{-1}{|I_e(\omega)|^2} \int_V d^3r \mathbf{E} \cdot \mathbf{J}_e^* \equiv \frac{1}{|I_e(\omega)|^2} [P_c + P_r + 2j\omega(W_m - W_e)], \quad (40)$$

where W_m and W_e are the magnetic and electric energies stored in the system, respectively. As can be seen from Eq. (40) the decrease in the input power of the impressed current goes into real power loss via the conductivity and the radiation through the wall, and into reactive power stored in the electromagnetic field. In our case, the corresponding impedance is^[18–29]

$$Z(\omega) = -\frac{1}{q_0^2} \int_{V_s} d^3r' E_z^{(1)}(r', z, \omega) J_0^*(r', z, \omega), \quad (41)$$

where V_s is the volume enclosing the current source, and $I_0(\omega)$ is the source spectral current, which is equal to $q_0 e^{-j\frac{\omega z}{\beta c}}$. Substituting for $E_z^{(1)}(r', z, \omega)$ and $J_0(r', z, \omega)$, the effective electrical impedance of the plasma-tube system as seen by the test charge is

$$Z(\omega) = -j I_0^2(\sigma_p a) \frac{\sigma_p^2}{\omega \epsilon_0 \epsilon_{33}} \frac{L_0}{2\pi} \left[\frac{K_0(\sigma_p a)}{I_0(\sigma_p a)} - F \right], \quad (42)$$

where L_0 is the length of a segment of the resistive cylindrical tube. For a perfectly conducting wall, such that $g \rightarrow \infty$, and in the absence of the plasma ($\omega_{pe} = 0$), we have $\eta = 0$, $\epsilon_{33} = 1$, $\sigma_p = \sigma_0$, and therefore, we obtain the following well known form of the space-charge impedance $Z_{(\omega_{pe}=0)}^{(g=0)}(\omega) \equiv Z^v = -j\chi_{c0}$,^[28,29]

$$\chi_{c0} = \frac{I_0^2(\sigma_0 a) \sigma_0^2}{\omega \epsilon_0} \frac{L_0}{2\pi} \left[\frac{K_0(\sigma_0 a)}{I_0(\sigma_0 a)} - \frac{K_0(\sigma_0 b)}{I_0(\sigma_0 b)} \right], \quad (43)$$

which shows that the effective impedance in the absence of plasma ($\omega_{pe} = 0$) and for a test charge motion of offset a in a cylindrical tube with a perfectly conducting wall is a negative reactance (pure capacitance) because χ_{c0} is positive for all the parameters. The resistive impedance of the tube wall $Z_w = R_w + j\chi_w$ is obtained from Eq. (42) by setting $\omega_{pe} = 0$ and then

subtracting the space-charge part of Eq. (43) from the resulting equation. To find the plasma impedance we firstly exclude the wall impedance by setting $g \rightarrow \infty$ ($\eta = 0$) in Eq. (42), and then subtract $Z^v(\omega)$ from the resulting equation to obtain the following formula for the plasma impedance $Z_{\text{plasma}}(\omega) = Z_p = R_p + j\chi_p$ with R_p and χ_p being the plasma resistance and reactance, respectively,

$$Z_p = -\frac{j I_0^2(\sigma_p a) \sigma_p^2 L_0}{2\pi \omega \epsilon_0 \epsilon_{33}} \left[\frac{K_0(\sigma_p a)}{I_0(\sigma_p a)} - \frac{K_0(\sigma_p b)}{I_0(\sigma_p b)} \right] - Z^v. \quad (44)$$

In the numerical results presented in the following, we use the following fixed values of $\nu = 0.2\omega_{pe}$, $b = 10$ cm, and $a = 1$ cm for the effective collision frequency, the cylindrical pipe radius, and the beam radius, respectively. In Fig. 2(a), the real part R_p of the effective plasma impedance per unit length of Eq. (44) is plotted versus ω_{pe}/ω for three different beam energies, namely, $\beta = 0.5$, $\beta = 0.7$, and $\beta = 0.9$. The curves of Fig. 2(a) show that the real part of the plasma impedance is a positive resistance with peak values at $\omega = \omega_{pe}$. The curves also show that the plasma resistance decreases with increasing the test charge energy.

The curves of Fig. 2(b) show the imaginary part χ_p of the plasma impedance versus ω_{pe}/ω for the source energies $\beta = 0.5$, $\beta = 0.7$, and $\beta = 0.9$. For a fixed ω , and varying ω_{pe} , the plasma reactance χ_p starts from zero value and becomes negative until it vanishes at $\omega_{pe} = \omega$. Therefore, for plasma frequencies ω_{pe} below ω , the plasma reactance χ_p is negative and capacitive in nature. The plasma reactance vanishes at the point $\omega_{pe} = \omega$, at which the plasma resistance R_p has its maximum value. For ω_{pe} above ω the plasma reactance becomes positive and inductive in nature.

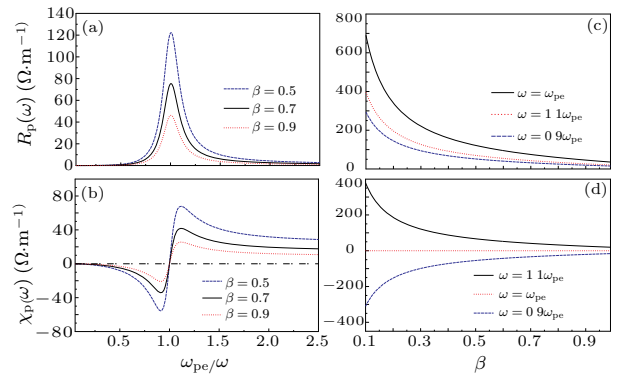


Fig. 2. Plasma resistance versus frequency with $\nu = 0.2\omega_{pe}$, $b = 10$ cm, and $a = 1$ cm for different beam energies.

In Figs. 2(c) and 2(d) the plasma resistance R_p and reactance χ_p are plotted versus the beam energy β for three different values of ω_{pe}/ω . The curves of Fig. 2(c) show that the plasma resistance decreases with increasing the test charge energy, as it has been observed in Fig. 2(a). The curves of Fig. 2(d) for χ_p versus energy show that the plasma reactance vanishes identically at $\omega_{pe} = \omega$, it is capacitive for $\omega_{pe} < \omega$ and

inductive for values of ω_{pe} above ω for all test charge energies.

The observations of Figs. 2(a)–2(d) show the same behavior of a parallel RLC resonator circuit which has the following equivalent impedance^[25]

$$Z_{\parallel}^{\text{RLC}}(\omega) = \frac{R_s}{1 + jQ(\frac{\omega}{\omega_0} - \frac{\omega_0}{\omega})} \equiv R(\omega) + j\chi(\omega), \quad (45)$$

where R_s , ω_0 , L , C , and Q are, respectively, the shunt resistance, the resonance frequency $\sqrt{1/LC}$, the inductance, the capacitance, and the quality factor $R_s\sqrt{C/L}$. The inductance and capacitance have dual ac characteristics, namely, the inductive reactance $\chi_L = \omega L$ is positive and is linear in frequency ω , whereas the capacitive one $\chi_C = -1/\omega C$ is negative and varies inversely with frequency. Here χ_L or χ_C may dominate depending on the frequency, or they may cancel each other out so that the parallel combination of L and C becomes an open circuit.

The plasma impedance shows the same characteristics of a parallel RLC resonator. The plasma admittance seen by the test particle can be written as the sum of the three admittances, namely,

$$Y^p = G^p + Y_L^p + Y_C^p, \quad Y^{\text{RLC}} = \frac{1}{R_s} + j\left(\omega C - \frac{1}{\omega L}\right).$$

Since the admittance is $-\infty$ as ω approaches zero, and is ∞ as ω approaches ∞ , the impedance curves approach zero at both ends of the frequency range due to the short-circuit action by the inductive part at low frequencies and the capacitive part at high frequencies. The inductive nature of the circuit dominates for $\frac{\omega_{pe}}{\omega} > 1$ and $\frac{\omega_0}{\omega} > 1$, while the capacitive nature is dominant for $\frac{\omega_{pe}}{\omega} < 1$, $\frac{\omega_0}{\omega} < 1$.

In response to external excitations, the knowledge of the plasma impedance as a function of frequency and plasma parameters allows for a better choice of the configuration of a microwave-plasma transmission system to couple waves to plasmas with high efficiency.^[30] Radio-frequency delivery systems are important components in semiconductor etch manufacturing tools. Understanding and stabilizing of the interaction of RF generators with plasmas is of the utmost importance for the design of an optimum RF powered plasma delivery system.^[31] The present work can be extended for tubes with corrugated walls or with a sharp jump in its cross section.^[32–34]

In conclusion, monopole electromagnetic fields induced in a cold and collisional plasma by a test charge drifting down a resistive cylindrical tube have been obtained. The plasma has been treated as an anisotropic dielectric medium with an effective diagonal permittivity tensor $\epsilon_p(\omega) \vec{I}$. The resistive and reactive parts of the plasma impedance seen by the test charge have been obtained analytically.

At wave frequencies near the electron plasma resonant frequency ω_{pe} , the plasma resistance and reactance evolve with frequency as in a parallel RLC resonator. The plasma resistance peaks at the electron plasma frequency, while the reactance can be capacitive or inductive in nature depending on the frequency

under consideration. The reactance starts from zero value and becomes negative until it reaches zero value at $\omega = \omega_{pe}$, where the plasma resistance has its maximum value, while it becomes positive and inductive in nature for ω_{pe} values below ω . It has also been observed that the plasma resistance decreases with increasing the test charge energy.

References

- [1] Johnson C 1965 *Field and Wave Electrodynamics* (New York: McGraw-Hill)
- [2] Shkarofsky I P et al 1966 *The Particle Kinetics of Plasmas* (New York: Addison-Wesley)
- [3] Kral N A and Trivelpiece A W 1973 *Principles of Plasma Physics* (New York: McGraw-Hill)
- [4] Boardman A D 1982 *Electromagnetic Surface Modes* (New York: Wiley)
- [5] Aliev Yu M et al 2000 *Guided-Wave-Produced Plasmas* (Berlin: Springer)
- [6] Trivelpiece A W and Gould R W 1959 *J. Appl. Phys.* **30** 1784
- [7] Popov O A 1990 *J. Vac. Sci. Technol. A* **8** 2909
- [8] Carl D A et al 1991 *J. Vac. Sci. Technol. B* **9** 339
- [9] Asmussen J and Mak P 1994 *Rev. Sci. Instrum.* **65** 1753
- [10] Gudmundsson T J and Lieberman M A 1998 *Plasma Sources Sci. Technol.* **7** 83
- [11] Iza F and Hopwood J 2005 *Plasma Sources Sci. Technol.* **14** 397
- [12] Chen F F 2006 *Plasma Sources Sci. Technol.* **15** 773
- [13] Barov N et al 2004 *Phys. Rev. Spec. Top. Accel. Beams* **7** 061301
- [14] Al-Khateeb A, Hasse R W, Boine-Frankenheim O and Hofmann I 2008 *New J. Phys.* **10** 083008
- [15] Zimmermann F 2004 *Phys. Rev. ST Accel. Beams* **7** 124801
- [16] Zenkevich P, Mustafin N and Boine-Frankenheim O 2002 *Proc. ECLLOUD 2002* (Yellow Report CERN-2002-001)
- [17] Chao A W 1993 *Physics of Collective Beam Instability in High Energy Accelerators* (New York: John Wiley & Sons)
- [18] Al-Khateeb A M, Hasse R W and Boine-Frankenheim O 2008 *Nucl. Instrum. Methods Phys. Res. Sect. A* **593** 171
- [19] Ng K Y 2006 *Physics of Intensity Dependent Beam Instabilities* (Singapore: World Scientific Publishing Co. pte. Ltd.)
- [20] Bawa'aneh M S and Boyd T J M 2007 *J. Plasma Phys.* **73** 159
- [21] Bawa'aneh M S, Al-Khateeb A M and Sawalha A S 2012 *Can. J. Phys.* **90** 241
- [22] Bawa'aneh M S, Al-Khateeb A M and Sawalha A S 2013 *IEEE Trans. Plasma Sci.* **41** 2496
- [23] Bawa'aneh M S, Ghada Assayed, Said M R and Al-Awfi S 2014 *Can. J. Phys.* **92** 504
- [24] Collin R E 1991 *Field Theory of Guided Waves* (New York: IEEE)
- [25] Pozar D M 1990 *Microwave Engineering* (New York: Addison-Wesley)
- [26] Dome G *Basic RF Theory, Waveguides and Cavities, CERN Yellow Reports, CAS-CERN Accelerator School and Rutherford Appleton Laboratory: Course on Rf Engineering for Particle Accelerators* (CERN 92-03 Vol.1, Geneva, Switzerland)
- [27] Jackson J D 1998 *Class. ElectroDyn.* 3rd edn (New York: Wiley)
- [28] Gluckstern R L 2000 *CERN Yellow Report* CERN 2000-011
- [29] Al-Khateeb A, Boine-Frankenheim O, Hasse R and Hofmann I 2005 *Phys. Rev. E* **71** 026501
- [30] Singh Pal K and Roy S 2007 *Appl. Phys. Lett.* **91** 081504
- [31] Brouk V and Heckman R 2004 *Stabilizing RF Generator Plasma Interact.: 47th Annu. Tech. Conf. Proceeding Soc. Vac. Coaters* (April 24–29 Dallas TX USA) p 49
- [32] Keil E 1972 *Nucl. Instrum. Methods* **100** 419
- [33] Levine J S 1984 *Int. J. Infrared Millimeter Waves* **5** 937
- [34] Al-Khateeb A, Boine-Frankenheim O, Plotnikov A, Shim, Y S and Hänichen L 2011 *Nucl. Instrum. Methods Phys. Res. Sect. A* **626** 1